Dynamic optimization of dry reformer under catalyst sintering using neural networks

Mazen Azzam[a], Nicolas Abdel Karim Aramouni[a], Mohammad N. Ahmad[a], Mariette Awad[b], Witold Kwapinski[c], Joseph Zeaiter[a],*

[a] *Department of Chemical and Petroleum Engineering, American University of Beirut, Lebanon*
[b] *Department of Electrical and Computer Engineering, American University of Beirut, Lebanon*
[c] *Department of Chemical Sciences, Faculty of Science and Engineering, Bernal Institute, University of Limerick, Ireland*
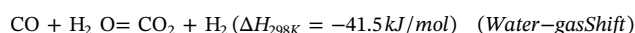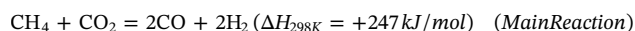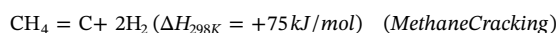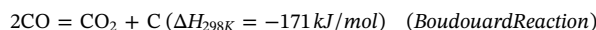
A B S T R A C T

Artificial neural networks (ANN's) have been used to optimize the performance of a dry reformer with catalyst sintering taken into account. In particular, we study the effects of temperature, pressure and catalyst diameter on the methane and CO_2 conversions, as well the H_2 to CO ratio and the molar percentage of solid carbon deposited on the catalyst. The design of the ANN was automated using a genetic algorithm (GA) with indirect binary encoding and an objective function that uses the effective number of parameters provided by Bayesian regularization. Results show that an industrially-acceptable catalyst lifespan for a dry reformer can be achieved by periodically optimizing temperatures and pressures to accommodate for the change in catalyst diameter caused by sintering. In particular, it was found that the reactor's operation favors high temperatures of almost 1000 °C, while the pressure must be gradually increased from 1 to 5 bars to remain as far as possible from carbon limits and ensure acceptable conversions and molar ratios in the syngas.

1. Introduction

The dry reforming of methane is a promising technology to convert the two main greenhouse gases – methane and carbon dioxide [1] – into syngas which can produce useful chemicals. In the dry reforming process methane reacts with CO_2 as an oxidant to produce syngas with a H_2/CO ratio close to unity, which makes it suitable for the synthesis of alcohols in the Fischer-Tropsch process [2,3]. This technology is an attractive option to valorize biogas produced in anaerobic digesters or landfills, with the annual biogas production reaching 59.0 billion cubic meters in 2013 [4], or in natural gas combined with a CO_2 capture or gas cleanup technology such as absorption [5], or in membrane separation [6], highlighting the huge potential feedstock for the process. The dry reforming process is an attractive technique to utilize greenhouse gases captured by gas separation processes. The main reactions governing the process are as follows:

$CH_4 + CO_2 = 2CO + 2H_2 \, (\Delta H_{298K} = +247 \, kJ/mol)$ (*Main Reaction*)

$CO + H_2O = CO_2 + H_2 \, (\Delta H_{298K} = -41.5 \, kJ/mol)$ (*Water−gas Shift*)

$CH_4 + H_2O = CO + 3H_2 \, (\Delta H_{298K} = +206 \, kJ/mol)$ (*Steam Reforming*)
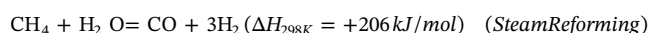
In addition to the carbon formation reactions:

$2CO = CO_2 + C \, (\Delta H_{298K} = -171 \, kJ/mol)$ (*Boudouard Reaction*)

$CH_4 = C + 2H_2 \, (\Delta H_{298K} = +75 \, kJ/mol)$ (*Methane Cracking*)

For a more comprehensive set of possible reactions see the work of Nikoo and Amin [7].

Despite its huge potential, dry reforming did not have any major industrial application, due to limitations concerning catalyst performance especially with carbon resistance [8–13]: supported nickel catalysts are the most widely used in industrial applications in reforming reactors, due to their low cost and good activity. Sehested [14] outlined four main shortcomings of nickel catalysts, namely: limited effectiveness, susceptibility to poisoning by sulfur and other elements, carbon formation and sintering at higher temperatures. In dry reforming processes, carbon formation and sintering are particularly problematic since they are related: compared to the steam reforming reaction [15] and the autothermal reforming reactions [16], the dry reforming reaction is the most endothermic and therefore requires the highest operating temperature to achieve satisfactory conversion. The low concentration of steam and the higher temperatures, in addition to the increased mole fraction of carbon in the process gases (high concentration of CO_2) cause an amount of carbon to build up on the catalyst. The literature is contradictory when it comes to describing carbon

formation on nickel catalysts: experimentally, three general types of carbon have been observed. Pyrolytic carbon forms essentially during thermal degradation of heavier hydrocarbons [8], while encapsulating carbon occurs especially in the presence of aromatic compounds and blocks the surface of the catalyst, preventing access to the active sites and causing a decrease in activity. Whisker carbon is the most dangerous type of carbon growth [7,17] due to its high strength which causes irreversible damage to the catalyst, including pellet breakage and detachment of active metal crystals. Its mechanism of formation has been the subject of numerous studies [18–20] and can be associated to the solubility of carbon in the nickel lattice. Carbon deposits diffuse through the nickel crystal and accumulate at the nickel/support interface from which a strong fiber grows and pushes the nickel crystal out. Still, most modeling works have assumed carbon to behave like graphite for equilibrium calculations [7,21–23]. In a previous work [24], we proposed a thermodynamic analysis for carbon formation derived from experimental measurements by Rostrup-Nielsen and Alstrup [25,26]. The diameter of the active metal particle has been found to affect the Gibbs energy of formation of carbonaceous species on the catalyst, with more carbon being formed on larger particles. Catalyst particles below the threshold value of 6 nm were found to accumulate very low amounts of carbon.

On the other hand, exposure of a supported catalyst to elevated temperatures over its service life causes it to suffer sintering, i.e. a loss of active surface area due to coalescence of the dispersed active metal particles [27], and thus an increase in active metal particle diameter over time. The temperature at which a material suffers from sintering is roughly dependent on its melting point, in addition to its Tamman and Huttig temperatures: At the Huttig temperature, atoms at crystal defects in the material experience mobility, while at the Tamman temperature, atoms in the bulk experience mobility. These temperatures for nickel are shown in Table 1.

Two main mechanisms describe the sintering of reforming catalysts [28]: at low temperatures, particle migration is the primary cause of sintering. The mobility of surface atoms and adatoms makes the center of the particle migrate on the catalyst surface, and collisions with other particles cause them to coalesce, and an increase in average particle diameter is exhibited. At higher temperatures, Ostwald ripening (atom migration) is responsible for an increase in the sintering rate. In reforming catalysts, the presence of steam in the gas above the catalyst increases sintering rate due to the mobility of Ni_2-OH dimers on the catalyst surface [29]. Sintering in these processes is mostly due to particle migration except at temperatures above 700–750 °C where Ostwald ripening becomes significant.

In addition to the activity loss that sintering causes, the increase in catalyst particle size with time decreases the Gibbs energy of formation of carbonaceous species and therefore an increase in carbon formation is expected. In this work, we employed artificial neural networks (ANN's) to model the dry reforming process, which is originally described by the Gibbs energy minimization method in [24]. Given a certain temperature, pressure and catalyst diameter, the model predicts the methane and CO_2 conversions, H_2/CO ratio and molar percentage of solid carbon deposited on the catalyst. This provides a faster method to estimate the outputs of the reactor. Next, we use the ANN model as an objective function to maximize the conversions and minimize carbon deposition and thus obtain optimal process conditions that change with the sintering of the catalyst.

Table 1
Sintering properties of nickel.

Property	Value
Melting point	1453 °C
Tamman temperature	581 °C
Huttig temperature	484 °C

2. Thermodynamic model

The dependence of carbon Gibbs energy of formation on the particle diameter has been studied by Alstrup [26] and the deviation from graphite thermodynamics ΔG_C^{dev} is given by:

$$\Delta G_C^{dev}(kJ/mol) = 2.6 + 93/d \tag{1}$$

with d being the particle diameter in nm.

Equilibrium compositions for given temperature and pressure are obtained by minimizing the total Gibbs free energy G^T of the multi-component system subject to conservation of mass constraints. In a given system of N chemical species, the total Gibbs energy G^T is given by:

$$G^T = \sum_{i=1}^{N} n_i(\Delta G_{fi}^0 + RT\ln(\overline{f_i}/f_{i,0})) \tag{2}$$

where ΔG_{fi}^0 is the standard Gibbs energy of formation of species i, $\overline{f_i}$ is the partial molar fugacity of species i at process conditions, $f_{i,0}$ is the standard state fugacity of species i, n_i is the number of moles of species i, R is the ideal gas constant, and T is the absolute temperature at process conditions.

The Gibbs energy of solid carbon G_C in this case is given by:

$$G_C = n_C(\Delta G_{f,Graphite}^0 + \Delta G_c^{dev}) \tag{3}$$

The total Gibbs energy of the reactive system is then the sum of the gas and solid phase Gibbs energies, assuming that the solid phase is only pure carbon:

$$G^T = \sum_{i=1}^{N-1} n_i(\Delta G_{fi}^0 + RT\ln(\overline{f_i}/f_{i,0})) + n_C(\Delta G_{f,Graphite}^0 + \Delta G_C^{dev}) \tag{4}$$

The problem statement becomes:

$$\min_{n_i} \quad G^T = \sum_{i=1}^{N-1} n_i(\Delta G_{fi}^0 + RT\ln(\overline{f_i}/f_{i,0})) + n_C(\Delta G_{f,Graphite}^0 + 2.6 + 93/d) \tag{5}$$

Details of the thermodynamic model and constraints are demonstrated in [24]. The problem is solved for temperatures between 700 and 1000 °C and pressures between 1 and 20 bars for various catalyst diameters. The temperature range was chosen based on the review of a large number of experimental and theoretical studies [30–35]. The carbon limits are defined here as conditions of temperature and pressure where carbon content exceeds 0.1 mol%. The initial molar composition of the reactive system is taken as 60% methane and 40% CO_2, as these values are an approximate representation of biogas composition.

Parameters studied are the methane and CO_2 conversions, defined as:

$$X_i = 100\left(\frac{n_{i,0}-n_{i,F}}{n_{i,0}}\right) \tag{6}$$

where X_i is the conversion of species i, and $n_{i,0}$, $n_{i,F}$ denote respectively the initial and final number of moles of species i. In addition, other parameters considered were the molar H_2/CO ratio and the carbon formation, expressed as a molar percentage C_s, and given by:

$$C_s = 100\left(n_{C,F}/\sum_{i=1}^{N} n_{i,F}\right) \tag{7}$$

3. Sintering model

At lower temperatures and in the presence of steam, the relation between average particle diameter $\overline{d}$ and time t is given in [14] by: